RELATIVISTIC BACKWARD WAVE OSCILLATORS: THEORY AND EXPERIMENT

B. Levush, T. Antonsen Jr., A. Bromborsky,[a] W. R. Lou, D. Abe, S. Miller,
Y. Carmel, J. Rodgers, V. Granatstein and W. Destler

Laboratory for Plasma Research
University of Maryland, College Park, MD 20742-3511

ABSTRACT

Microwave sources based on backward-wave oscillators with relativistic electron beams are capable of producing high power coherent radiation in the cm and mm wavelength regime. Although there have been a number of experiments reported over the last decade on this topic, there are only a few publications providing a theoretical description of these devices. Thus, there is a need for theoretical models which can be compared in detail with the experimental data. This work is devoted to fill this need. The linear and nonlinear theory of backward-wave oscillators is developed taking into account reflection of the electromagnetic wave at the boundaries of the slow wave structure. The effects of finite duration and rise time of the electron beam pulse on device operation are discussed.

INTRODUCTION

One of the most successful examples of high power microwave sources utilizing high current relativistic electron beam is the Backward-Wave Oscillator (BWO). The device consists of a periodic metallic structure into which a high current relativistic electron beam is injected. The beam is usually confined by a strong axial magnetic field. The slow wave structure reduces the phase velocity of electromagnetic (EM) waves below the vacuum speed of light so that the electrons in the relativistic beam can give up energy directly to one of the eigenmodes of the structure.

The theoretical model which we used to simulate the operation of the BWO is an extension of the model published in Ref. [1], which is essentially the same as has been studied in connection with traveling wave devices for decades [2]. The model can be described as follows. An electron beam which is injected into a slow wave structure interacts weakly with an electromagnetic wave of the vacuum (or cold) structure. The interaction is weak in the sense that, if examined over a region of space of the size of the order of one period of the structure, the electromagnetic field has the temporal and spatial dependences of a wave in the empty structure. The effect of the beam is to cause the electromagnetic wave to vary slowly in time and axial distance. Further, the beam induces a relatively small space charge field which is proportional to the beam density. However, the model in [1] assumes that the backward propagating wave after interacting with the beam leaves the system without reflections. In practice, the backward wave suffers reflection at the beam entrance of the cavity (where it is cut off by a drift tube) and becomes a forward wave. The forward wave does not interact with the beam, but it may be reflected at the beam exit of the periodic structure. The reflected forward wave becomes a backward wave which can interfere constructively or destructively with amplified backward wave. This is illustrated in Fig. (1). In a realistic structure, the total round trip

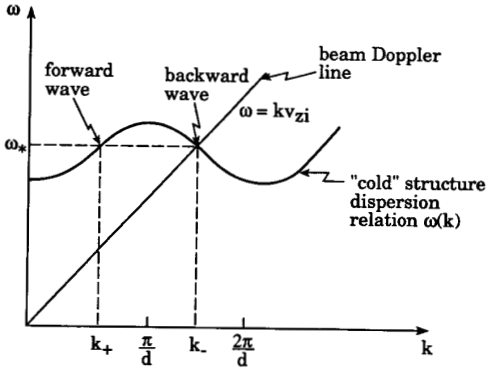

Figure 1. A schematic picture of a dispersion relation, $\omega(k)$, of TM_{01} mode in an infinitely long periodic structure. The straight line which intersects the cold structure dispersion curve is the electron beam Doppler line, $\omega = kv_{zi}$, where v_{zi} is the beam initial velocity. The wave number k_- denotes the backward wave and k_+ denotes the forward wave, while the frequency for both waves is the same, ω_*.

CH3075-9/91/0000-0775 $1.00 © 1991 IEEE

amplitude reflection coefficient can be in excess of 70% and, thus, can be expected to influence the operation of the device.

In Ref. [3] we extended the theory for a relativistic BWO of a finite length developed before by taking into account the effect of reflections of the electromagnetic wave at both boundaries of the interaction region. We used this theory to simulate the operation of University of Maryland BWO.

STARTING CURRENT CALCULATION AND MEASUREMENT

The starting current is the minimum beam current required to start oscillations from noise in the RF structure. The expression for the starting current for a cold beam in our notation takes the form

$$I_{st} = \frac{I_A}{4\pi}\left(\frac{d}{L}\right)^3 \frac{\gamma_i^3\beta_{zi}^2}{(k_* d)}\frac{\beta_g(\omega_*)}{C(r_b,\omega_*)}\tilde{I}_{st}, \qquad (1)$$

where $I_A = mc^3/q = 1.7\times 10^4 Amps$, L is the total length of the structure in cm, d is the period of the structure in cm, and γ_i and $\beta_{zi} = (1-1/\gamma_i^2)^{-1/2}$ are the relativistic factor and normalized axial velocity of the injected beam. The resonant frequency, ω_*, appearing in Eq. (1), is defined as the intersection of the dispersion curve $\omega(k_-)$ (k_- is the wave number of the backward wave) of the cold slow wave structure and the electron beam Doppler line $\omega = kv_{zi}$, where $v_{zi} = c\beta_{zi}$, see Fig. (2). This also determines the resonance wave number $k_* = \omega_*/v_{zi}$ and the group velocity $\beta_g(\omega_*)$.

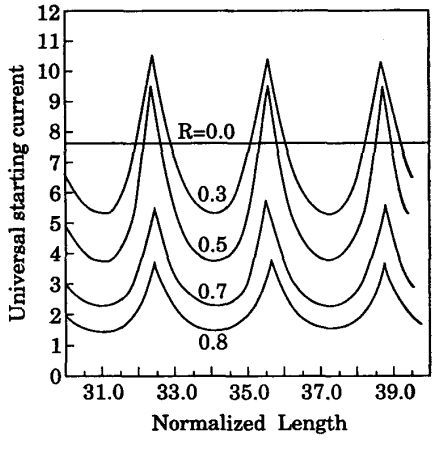

Figure 2. The "universal" starting current (I_{st}) versus the normalized length ($k_*L = \omega_*/v_{zi}L$) for five values of the combined reflection coefficient, R = 0.0, 0.3, 0.5, 0.7, 0.8.

The coupling coefficient $C(r)$ is defined as

$$C(r) = \frac{\left|\int_0^d \frac{dz}{d} E_{zp}(z,r)\right|^2}{\int_0^d \frac{dz}{d}\int_0^{r_w(z)} \frac{2\pi r dr}{d^2}\{|\mathbf{E}_p(r,z)|^2 + |\mathbf{B}_p(r,z)|^2\}}, \qquad (2)$$

where $r_w(z)$ is the wall radius of the periodic structure, $\mathbf{E}_p(r,z)$ and $\mathbf{B}_p(r,z)$ are the complex amplitudes for the electromagnetic fields which represent the solutions for waves in the empty structure.

The coupling coefficient $C(r = r_b)$ is the measure of strength of the axial electric field component which couples with the beam. The coupling coefficient depends on the EM fields in the "cold" structure, therefore it can be calculated and tabulated separately as a function of r and k_* for a given structure.

The quantity $\tilde{I}_{st}$ is a dimensionless number which we refer to as the "universal" starting current. Thus, the dependence of the actual starting current on physical parameters of the device enters through the factors multiplying $\tilde{I}_{st}$. Note that Pierce parameter C_p commonly used in the microwave device literature, [2], is related to our normalized parameters via

$$\tilde{I} = (C_p k_* L)^3. \qquad (3)$$

When reflections of the EM wave are included Eq. (1) remains valid, however, the "universal" starting current now depends on the magnitude of the reflection coefficient, $R = \rho_0\rho_L$, and the total round trip phase change, $2k_*L + \phi_r$, at frequency ω_* for the EM wave. The quantities $\rho_0\exp(i\phi_0)$ and $\rho_L\exp(i\phi_L)$ are the complex reflection coefficients at the left and right boundaries of the slow wave structure, respectively. The quantity ϕ_r is the combination of the phases ϕ_0 and ϕ_L, $\phi_r = \pi - \phi_0 - \phi_L$. We have determined $\tilde{I}$ versus R dependence via numerical solution of the nonlinear equations, derived in [3], in the linear regime. The results are shown in Fig. (2) where the "universal" start current versus the device normalized length k_*L for five different values of the combined reflection coefficient are plotted. Here we have set $\phi_r = 0$, but for a different value of ϕ_r the same plot can be applied by redefining the k_*L axis in the plot, $k_*L_{new} = k_*L + \phi_r/2$, which will shift the plot in Fig. (2) along the abscissa. For $R = 0$ the "universal" start current, $\tilde{I}_{st}$, versus the normalized length, k_*L, is a constant and equal to 7.7 confirming previous results [1],[4]. As can be anticipated, for larger R (higher cavity quality factor, Q) the "universal" starting current tends to decrease and exhibits a periodic dependence on the parameter k_*L. This periodic behavior is due to the interference between the amplified and reflected waves. For frequencies for which constructive interference takes place it is easier to start the oscillations than for frequencies for which destructive interference occurs.

For a fixed length of the slow wave structure variations

in k_*L result from variations in beam energy through the dependence of k_*L on the beam velocity. Recall that k_* is determined by the intersection of the beam and structure dispersion curves. Thus, the reflections make device starting conditions a sensitive function of diode voltage.

We used the results of our analysis to calculate the starting current versus electron gun voltage in the RF structure used in our experiment.

The structure used in the experiment was a circularly symmetric waveguide with average radius, r_{av}=1.5 cm, and sinusoidal ripples of period d = 1.67 cm and height $\Delta = (r_{max} - r_{min})$= .82 cm. The structure was 8 periods long with a drift tube at the beam entrance end and a gentle taper to an overmoded waveguide at the beam exit end. The dispersion curves, coupling coefficients, and reflection coefficients were calculated using a separate code [5]. In Fig. (3) a plot of start current versus diode voltage for the structure is shown.

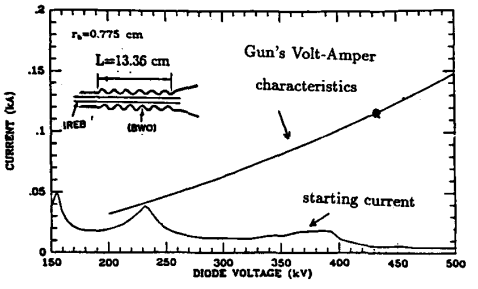

Figure 3. (a) The starting current in kA versus diode voltage in kV for the RF structure used in the experiment; (b) Volt-Ampere characteristic of the electron gun. The solid dot is the point below which no radiation from BWO was observed.

We observe that the maximum starting current is about 50 Amps and the minimum is about 5 Amps. This start current is much smaller than the current which is typically used in the device. A series of low current experiments attempting to measure the start current have been conducted.

The main challenge in the experiment was to achieve BWO operation over a wide range of electron beam energy and current. Since for a particular gun geometry the variation in the beam current is limited, we built a number of electron guns which allowed us to cover a broad range of beam parameters. The Volt-Ampere characteristics of one such gun is shown in Fig. 3. The black dot marked on the curve indicates the parameters of the BWO (I_{max}=113 Amp and V_{max}=440 kV) for which the theoretical predictions are compared with the experimental data. This is the current below which no radiation has been detected with the available detectors. We find that the "measured starting current" is above the calculated starting current. However, the starting current is defined under the assumption that the flat top of the electron beam pulse is infinitely long. In a typical BWO experiment the voltage and the current pulse have a finite duration with a finite rise time. For example, Fig. 4a shows the oscilloscope traces of the electron beam current and voltage for the case labeled by the dot on the Volt-Ampere line in Fig. 3. Figure 4b shows the corresponding oscilloscope trace of the radiated power. The simulations were performed with the experimentally measured waveforms for voltage and current, and the results for the radiation output power in normalized units versus time are shown in Fig. 5. We also included in the simulations the time-dependence of the voltage depression of the electron beam and the A.C. space-charge effect. The maximum calculated efficiency is 20%, while the measured

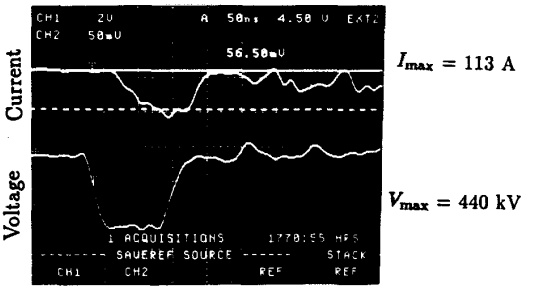

Figure 4a. The beam current versus time (upper trace) and the beam voltage (lower trace).

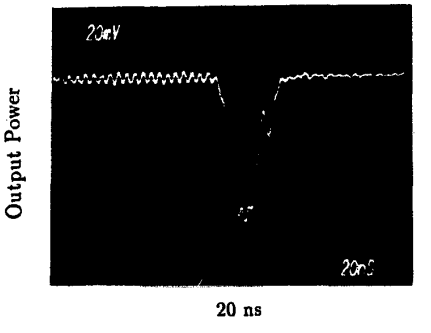

Figure 4b. The oscilloscope trace of the radiated power.

efficiency is 15%-25%. When a slightly lower current (90 Amps) is used in the simulation, the maximum power is reduced by a factor of five. This shows that the time-dependent start current calculation is in a better agreement with the experiment.

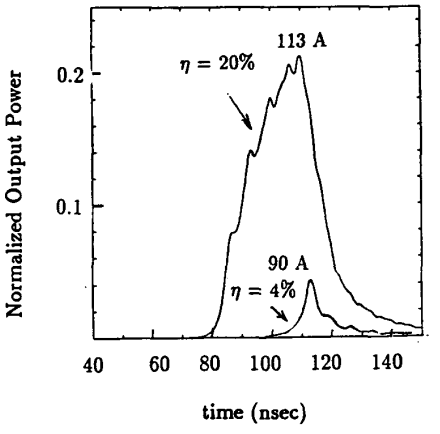

Figure 5. The normalized output power versus time in nsec for maximum current (a) 113 Amp and (b) 90 Amp. The corresponding efficiency is (a) 20% and (b) 4%.

SUMMARY

We have adopted the approach which has been developed for the description of microwave devices such as TWT's, gyrotrons, ubitrons, and BWO's to the case of relativistic BWO's with internal reflections. The description of the model is presented in Ref. (3). This model predicts the mode jumping effect during the voltage rise, which has been observed recently in the experiments [6]. In future work we will include the effects of the finite axial magnetic field and excitation of the higher order transverse modes which have been observed experimentally.

ACKNOWLEDGEMENT

This work has been partially supported by the U.S. Army Harry Diamond Laboratories.

REFERENCES

[a] Harry Diamond Laboratories

[1] N. S. Ginzburg et al., *Sov. Radiophys. and Electron.*, vol. 21, 728, 1979.

[2] J. R. Pierce, "Traveling-wave tubes," D. Van Nostrand Comp., Toronto, 1950.

[3] B. Levush et al., submitted IEEE Trans. on Plasma Science, special issues on high power microwave generation, 1992.

[4] J. A. Swegle, *Phys. Fluids*, vol. 30, 1201, 1987.

[5] A. Bromborsky and B. Ruth, *IEEE Trans. Microwave Theory Tech.*, MTT-32, 600, 1984.

[6] Y. Carmel and W. Lou, private communication.